In-situ and Laboratory Cyclic Response of an Alluvial Plastic Silt Deposit

Réponse cyclique in situ et en laboratoire d'un gisement de limon plastique alluvial

Ali Dadashiserej, Amalesh Jana, **Armin W. Stuedlein** & T. Matthew Evans
School of Civil and Construction Engineering, Oregon State University, USA, Armin.Stuedlein@oregonstate.edu

Benchen Zhang, Zhongze Xu, & Kenneth H. Stokoe II
Department of Civil, Architectural, and Environmental Engineering, University of Texas, Austin, USA

Brady R. Cox
Department of Civil and Environmental Engineering, Utah State University, USA

ABSTRACT: Current best practices for the assessment of the cyclic response of plastic silts are centered on the careful sampling and cyclic testing of natural, intact specimens. Side-by-side evaluation of *in-situ* and laboratory element test responses are severely limited, despite the need to establish similarities and differences in their characteristics. In this paper, a coordinated laboratory and field-testing campaign that was undertaken to compare the strain-controlled cyclic response of a plastic silt deposit at the Port of Longview, Longview, WA is described. Following a discussion of the subsurface conditions at one of several test panels, the responses of laboratory test specimens to resonant column and cyclic torsional shear testing, and constant-volume, strain-controlled cyclic direct simple shear testing are described in terms of shear modulus nonlinearity and degradation, and excess pore pressure generation with shear strain. Several months earlier, the in-situ cyclic response of the same deposit was investigated by applying a range of shear strain amplitudes using a large mobile shaker. The *in-situ* response is presented and compared to the laboratory test results, highlighting similarities and differences arising from differences in mechanical (e.g., constant-volume shearing; strain rate-effects) and hydraulic (e.g., local drainage) boundary conditions and the spatial variability of natural soil deposits.

RÉSUMÉ : Les meilleures pratiques actuelles pour l'évaluation de la réponse cyclique des limons sont centrées sur l'échantillonnage minutieux et l'analyse cyclique d'échantillons de laboratoire naturels et intacts. L'évaluation côte à côte des réponses aux tests sur les éléments in situ et en laboratoire est très limitée, malgré la nécessité d'établir des similitudes et des différences dans leurs caractéristiques. Cet article décrit une campagne coordonnée de tests en laboratoire et sur le terrain entreprise pour comparer la réponse cyclique contrôlée par la déformation d'un dépôt de limon plastique au port de Longview, Longview, WA. Suite à une discussion des conditions souterraines sur l'un des nombreux panneaux de test, la réponse des éprouvettes de laboratoire au cisaillement de torsion de la colonne résonnante et au test de cisaillement simple cyclique direct à volume constant contrôlé par déformation est décrite en termes de dégradation du module de cisaillement et de pore génération de pression avec déformation de cisaillement. Ensuite, la réponse cyclique in situ du même dépôt soumis à diverses amplitudes de déformation de cisaillement appliquées par un grand agitateur mobile est présentée et comparée aux résultats des tests de laboratoire, mettant en évidence les similitudes et les différences résultant de différences mécaniques et les réponses du système hydrauliques.

KEYWORDS: *in-situ* cyclic testing, cyclic and dynamic laboratory tests, excess pore pressure, shear modulus reduction

1 INTRODUCTION.

Characterization of the cyclic response of plastic, fine-grained soils has generally focused on reconstituted and natural, intact laboratory specimens. Such studies have allowed the quantification of critical dynamic soil properties and behaviors, including the: (1) threshold shear strain at the departure from linear-elastic behavior, γ_{te}, (2) threshold shear strain at which the generation of residual excess pore pressure begins, γ_{tp} (Hsu and Vucetic 2006; Tabata and Vucetic 2010; Ichii and Mikami 2018; Jana and Stuedlein 2021a), (3) variation of the cyclic resistance ratio, *CRR*, with the number of uniform cycles, *N* (e.g., Wijewickreme et al. 2019, Jana and Stuedlein 2021a), and (4) shear modulus reduction and damping curves (e.g., Vucetic and Dobry 1991). Geotechnical earthquake engineering practice relies on these and similar studies to support the selection of important models of material behavior for use in site response and numerical deformation analyses.

The characterization of such critical dynamic responses *in-situ* offers several advantages over laboratory testing which include: (1) significantly larger volumes of soil may be tested compared to small laboratory specimens, (2) the drainage characteristics of a given deposit, and possible interaction with other deposits, are operative and may be observed (Adamidis and Madabhushi 2018, Jana and Stuedlein 2021b, 2021c), and (3) soil deposits can be tested under *in-situ* conditions (e.g., degree of saturation, S_r)avoiding back-pressure saturation of laboratory specimens, which can lead to softer responses than that in the field for partially-saturated soils. Kurtulus and Stokoe (2008) applied cyclic loading to a drilled shaft foundation and observed the partially-saturated, non-plastic silt response to vertically-polarized shear waves to quantify γ_{te} and the variation of shear modulus, *G*, with shear strain, γ. Cox et al. (2009) used a large mobile shaker (i.e., vibroseis) to perform staged dynamic loading of a silty sand deposit 3 to 4 m below the surface in order to quantify γ_{tp} and the variation of shear modulus, *G*, and residual excess pore pressure ratio, $r_{u,r}$, with shear strain, γ. Jana and Stuedlein (2021b, 2021c) used controlled blasting to quantify γ_{te}, γ_{tp}, and the variation of *G* and $r_{u,r}$ with γ at a depth of 11 and 25 m in a plastic silt and medium dense sand deposit, respectively. Roberts et al. (2016) used a vibroseis to quantify γ_{te}, γ_{tp}, and the variation of *G* and $r_{u,r}$ with γ within loose and dense clean sands and loose, nonplastic silty sands. These soils are difficult to sample; *in-situ* testing yielded valuable dynamic soil behavior without the need for soil freezing and coring.

In this paper, a coordinated cyclic laboratory and *in-situ* testing campaign conducted on the alluvial, plastic silts comprising one of several test panels at Barlow Point, a property situated along the Columbia River and part of the Port of Longview, Longview, WA (USA) is summarized. The laboratory investigation included cyclic direct simple shear and resonant column cyclic torsional shear tests on intact, natural specimens, the results of which are compared to the *in-situ* dynamic response evaluated with an instrumented array of sensors and the staged vibroseis shaking. Differences and similarities in the responses of the plastic silt obtained through this field and laboratory testing are described and point to several advantages offered by *in-situ* dynamic testing of these plastic silt soils.

2 SITE AND SUBSURFACE CHARACTERIZATION

The focus in this paper is the test program at test panel UT-2 which is set within the context of a larger *in-situ* test program at the Port of Longview. The larger program included several vibroseis test panels and one controlled blasting test panel. Subsurface explorations were conducted to characterize each test panel, including cone penetration tests (CPTs), mud-rotary borings with thin-walled and split-spoon sampling, and standard penetration tests (SPTs), and small-strain seismic tests (i.e., spectral-analysis-of-surface-waves, downhole, and direct-push crosshole seismic tests). The site and exploration plan in the proximity of UT-2 is presented in Figure. 1. A cross-section of the conditions in proximity to test panel UT-2 and the instrumented array used to observe the dynamic response to *in-situ* cyclic testing with the University of Texas, Austin, T-Rex mobile shaker are presented in Figure 2. The subsurface conditions were identified using soil samples and the Soil Behavior Type Index, I_c, (Robertson 1990) and consist of dense, silty sand with gravel fill to a depth ranging from 0.4 to 0.6 m, overlying a layer of alluvial, interbedded, medium stiff sandy silt and clayey silt to silty clay with sand. This layer transitioned to a deep layer of, very soft to soft clayey silt (ML) fining to clayey silt to silty clay and clay (MH to CH) with traces of sand and woody debris. The instruments comprising the array at UT-2 are shown to scale and located approximately 10 m east of the north-south Section A-A' (Figures 1 and 2). The groundwater table (GWT) was measured at a depth of 1.5 m, and was known to vary approximately +/- 0.5 m across the site.

The average corrected cone tip resistance, q_t, and soil behavior type index, I_c (Robertson 2009), over the range in instrumented depths (i.e., 1 to 2.5 m) are equal to 0.8 MPa and 2.63, respectively. The SPTs confirm the generally very soft to soft nature near the instrumented array. Direct-push crosshole tests were conducted approximately 5 m west of UT-2 following the procedures outlined in Cox et al. (2018) and indicated that the compression wave velocity, V_p, ranged from about 270 m/s at the GWT depth of 1.5 m to 650 m/s at a depth of 2.0 m below the ground surface. At a depth of 2.5 m to the final measurement depth of 4.3 m, V_p, varied between 1400 and 1500 m/s. Based on the V_p measurements, the depth to essentially full saturation of the plastic soils at UT-2 is approximately 2.5 m (1.0 m below GWT). However, based on Stokoe et al. (2016), silty sands that exhibit V_p greater than about 700 m/s tend to exhibit a degree of saturation above 99.5% and behave as fully-saturated in terms of excess pore-water pressure generation. The shear wave velocity, V_s, generally decreased with depth and was equal to approximately 100 m/s within the depths of the embedded instrumented array (i.e., 1.0 to 2.5 m).

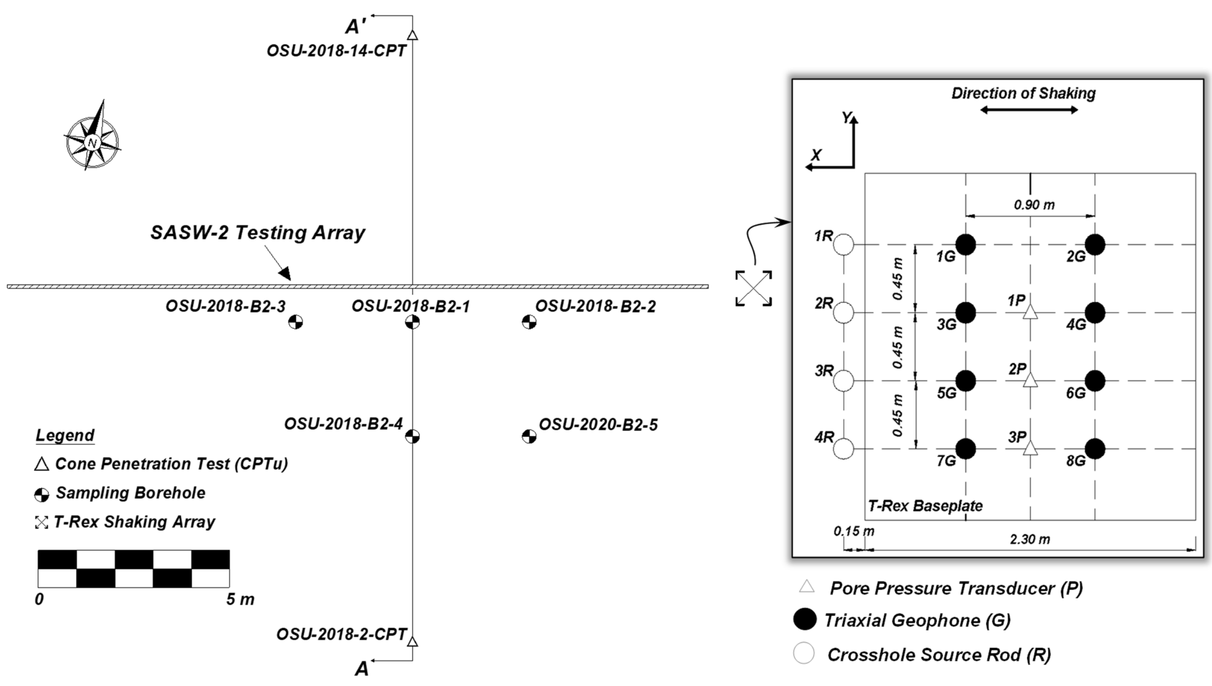

Figure 1. Site and exploration plan at test panel UT-2; inset figure presents the plan view of instruments within the T-Rex loading footprint. Section A-A' is shown in Figure 2.

3 LABORATORY TEST PROGRAM

3.1 *Cyclic Direct Simple Shear (DSS) Test Program*

Laboratory tests were conducted on disturbed samples and intact specimens prepared from thin-walled tube samples retrieved from a mud-rotary borehole OSU-2020-B2-5 (Figures 1 and 2) advanced in proximity to the UT-2 T-Rex shaking array. The laboratory element tests described in this study were performed using a SSH-100 GCTS cyclic DSS with retrofitted platens to accommodate bender element (BE) and piezoelectric disc (PD) transducers, which provide indications of specimen quality and S_r of natural, intact specimens (Landon et al. 2007, Jana and Stuedlein 2021a). The cyclic test procedure was designed to replicate the *in-situ*, staged, dynamic loading applied by the T-Rex vibroseis (described below) to test panel UT-2. The constant-volume, staged, strain-controlled cyclic tests used the same number of loading cycles, N, and the shear strain amplitudes were similar to the *in-situ* tests. Following consolidation under the *in-situ* vertical effective stress, $\sigma'_{v0} = \sigma'_{vc} \approx 44$ kPa including the additional vertical stress imposed by T-Rex, body wave velocity measurements were made and the constant-volume, strain-controlled cyclic phase commenced using 40 cycles of uniform shear strain amplitude at 0.1 Hz loading frequency, f (f = 10 Hz for T-Rex loading). Following completion of the cyclic phase, specimens were recentered in the DSS device and reconsolidated to σ'_{vc}, followed by the next strain-controlled cyclic phase with a larger shear strain amplitude. The sequence of cyclic loading, recentering, and reconsolidation of DSS test specimens simulates the *in-situ*, staged, T-Rex loading applied at test panel UT-2. Table 1 summarizes the properties of specimens subjected to the staged, strain-controlled and RCTS tests.

Table 1. Summary of specimen properties for laboratory element tests.

Test ID	Depth (m)	*In-situ* Vert. Eff. Stress, σ'_{v0} (kPa)	Void Ratio e_c	Degree of Saturation S_r[2] (%)	Over-consolidation Ratio OCR	Plastic Index *PI*	Fines Content *FC* (%)	USCS Soil Class.	Shear Wave Velocity V_s (m/s)	Compression Wave Velocity V_p (m/s)
DSS-T1	1.42	43	4.10[1]	~100	2.67	26	99	MH	89	1,162
DSS-T2	1.45	44	1.70	~100	2.61	22	100	CL	119	1,213
RCTS-T1	1.22	29[2]	1.78	90.8	-	19	87	MH	92	208[3]

[1] woody debris within the specimen skewed the computation of void ratio.
[2] determined from gravimetric and volumetric measurements.
[3] measured under effective *in-situ* confining pressures under the T-Rex load.

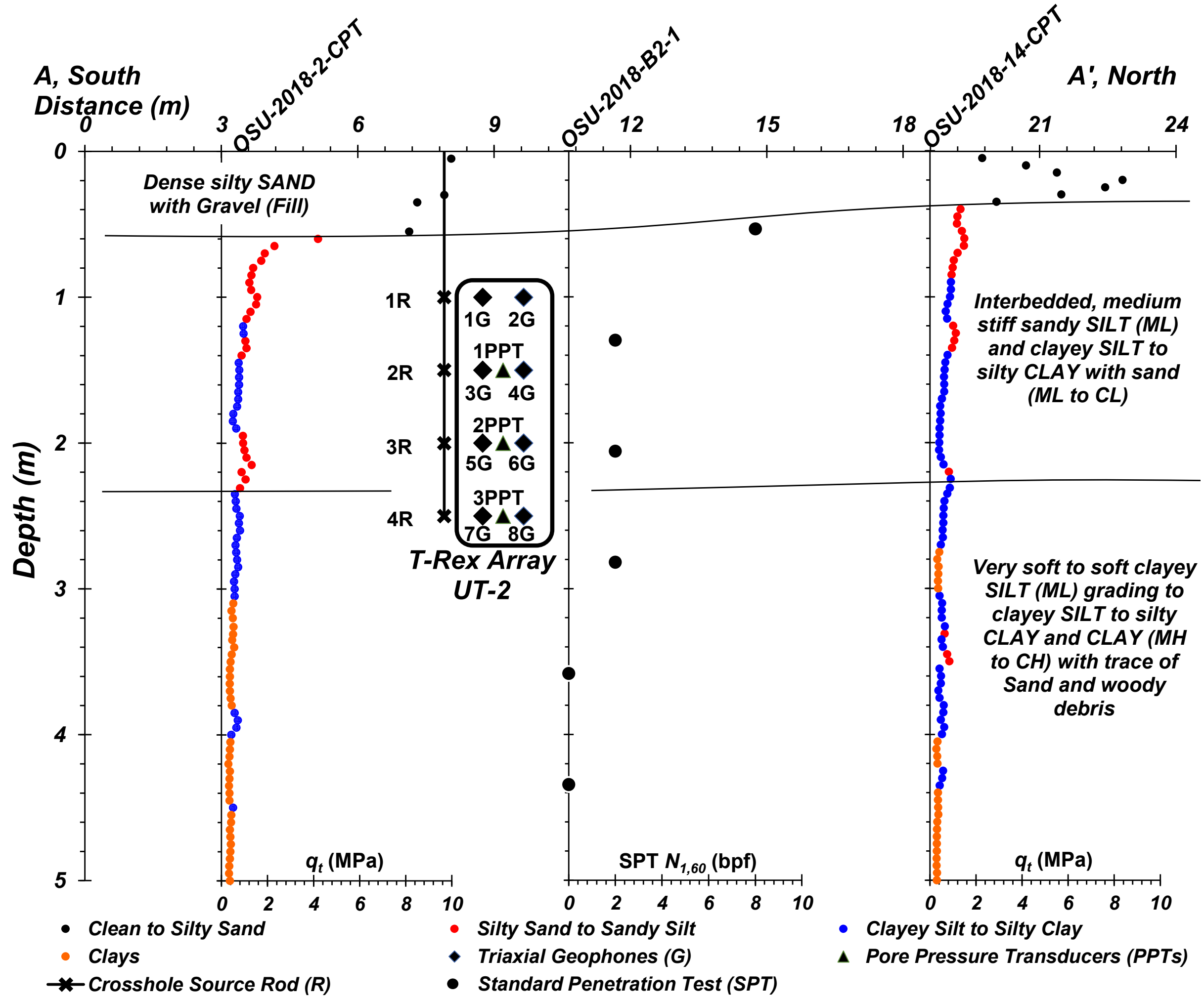

Figure 2. Subsurface conditions along Section A-A' in proximity to instrumented array UT-2, situated 10 m east (out of plane) of Section A-A'.

Figure 3 presents the results of Specimen DSS-T2 subjected to three stages of constant-volume, strain-controlled cyclic loading in terms of the normalized shear stress-shear strain hysteresis, τ_{cyc}/σ'_{vc}, excess pore pressure ratio, r_u, residual r_u, defined as r_u at end of a given loading cycle, $r_{u,r}$ (Hsu and Vucetic 2006), and the variation of normalized shear modulus, G/G_{max}, versus shear strain. The generation of negative excess pore pressure in the first quarter-cycle of loading observed for each

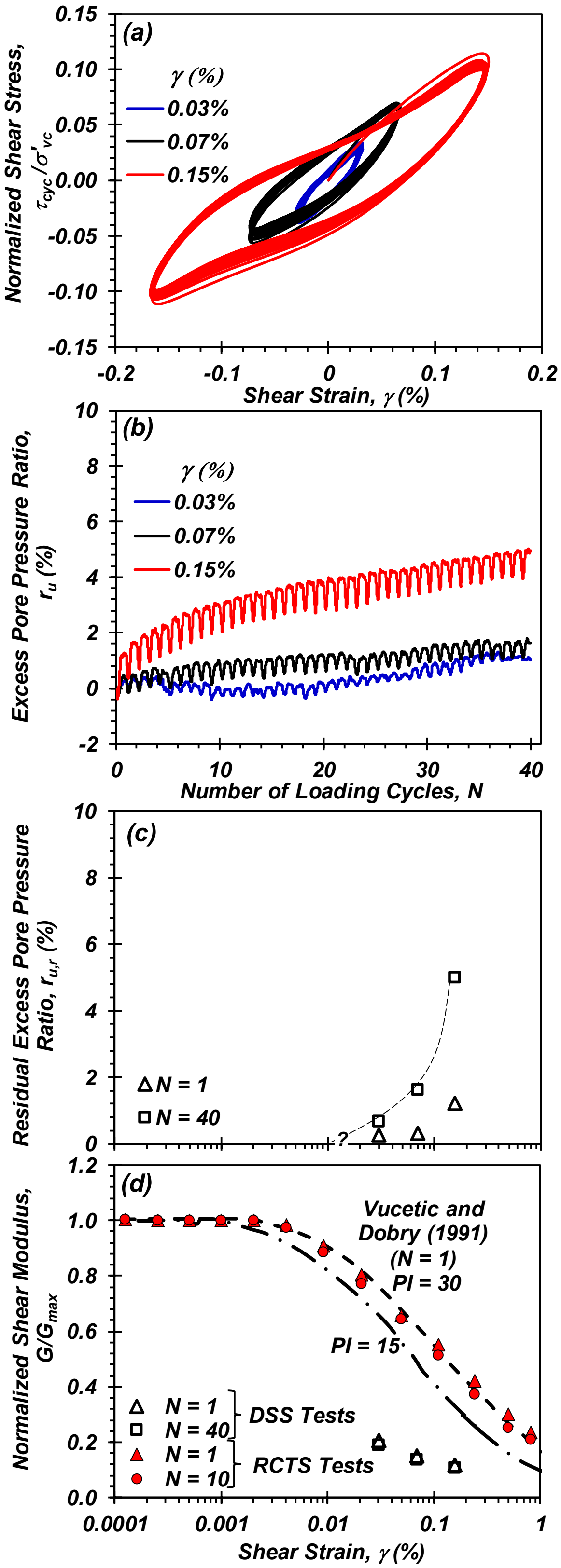

Figure 3. Cyclic response of selected specimens: (a) τ_{cyc}/σ'_{vc} -γ hysteresis, and variation of: (b) r_u with N, (c) $r_{u,r}$ with γ for $N = 1$ and 40, and (d) G/G_{max} with γ and comparison to Vucetic and Dobry (1991).

shear strain amplitude (Figure 3b) is due to the margin of overconsolidation exhibited by the intact specimens (Table 1). This initial response, followed by the accumulation of positive excess pore pressure in the cycles of loading that follow, is consistent with the pore pressure responses of natural plastic soils reported by Matasovic and Vucetic (1995) and Jana and Stuedlein (2021a). Figure 3c presents the variation of $r_{u,r}$ with γ, suggesting that γ_{tp} = is on the order of 0.01 to 0.02%.

The secant shear modulus, G_{sec}, is calculated from the slope of a fitted line connecting the maximum absolute positive and negative shear strains in the τ_{cyc}/σ'_{vc} hysteresis for each cycle (Figure 3a), whereas G_{max} is determined based on the V_s measured using bender elements under a 20 Hz square wave. Degradation of G with increases in γ and N is observed in Figure 3d because of the buildup of positive excess pore pressure and reduction in σ'_v. The slight difference in G/G_{max} between $N = 1$ and 40 stems from the relatively small changes in r_u as N increases (Figure 3b). The deviation between the DSS test-derived and Vucetic and Dobry (1991) G/G_{max} curves result in part from the loading frequency (0.1 Hz) used, possible apparatus compliance, and differences in S_r. The effect of S_r and correction for strain rate-effects is described below.

3.2 *Resonant Column-Torsional Shear Test Program*

One high-plasticity (i.e., elastic) silt, resonant column-torsional shear specimen RCTS-1 (Table 1) was prepared from a thin-walled tube sample taken adjacent to the UT-2 test panel. The loading protocol consisted of the staged application of, and consolidation under, isotropic confining pressures, σ'_c, of 7, 14, 28, 56, and 112 kPa. Following each consolidation stage, strain-controlled cyclic loading with $\gamma = 0.0005\%$ was applied and V_s measured (Table 1). Small-to-large strain cyclic loading was then applied at selected confining pressures and a frequency of 0.5 Hz. Figure 3d presents the results for $\sigma'_c = 28$ kPa, indicating $\gamma_{te} \approx 0.004\%$ and generally following the Vucetic and Dobry (1991) G/G_{max} curve for $PI = 30$, consistent with its MH classification. Comparison to the strain-controlled Specimen DSS-T2 suggests that apparatus compliance, rather than strain rate-effects, provides the dominant factor explaining the apparently low G/G_{max} data derived from the DSS test. However, the variability of the soil in proximity to the UT-2 array was noted to be relatively large and typical of alluvial deposits: the DSS and RCTS test specimens were developed from boreholes that were separated by approximately 10 m, and local differences in the soil conditions may also serve to explain some of the differences in shear modulus characteristics noted here.

4 *IN-SITU* CYCLIC TESTING USING THE T-REX MOBILE SHAKER

In-situ dynamic testing of test panel UT-2 was performed using the large mobile shaker T-Rex. The mobile shaker can apply horizontal cyclic loading at the ground surface to produce vertically-propagating, horizontally-polarized shear waves (S_{VH}-waves) with varying amplitude travelling within a soil deposit, allowing observation of particle velocities and excess pore pressures to deduce the dynamic soil response (Cox et al. 2009; van Ballegooy et al. 2015; Roberts et al. 2016). The *in-situ* observations at UT-2, made using seven stages of loading (Table 2), facilitate the comparison to the laboratory test results described previously to identify the similarities and differences of the cyclic soil response including the triggering of excess pore pressure, onset of nonlinear behavior, and degradation of soil stiffness.

Table 2. Loading stages applied using T-Rex at UT-2.

Loading Stage and Number of Cycles, N	Voltage	Average Cauchy Shear Stain at 1PPT	Average Cauchy Shear Stain at 2PPT
Stage 1, N = 40	0.25	0.001	0.001
Stage 2, N =40	0.50	0.008	0.003
Stage 3, N =40	1.0	0.017	0.009
Stage 4, N =40	1.5	0.028	0.016
Stage 5, N =40	2	0.055	0.037
Stage 6, N =40	3	0.134	0.082
Stage 7, N =100	5	0.261	0.175

4.1 *Instrumentation Program and Test Procedure*

Observation of the *in-situ* dynamic, coupled, excess pore pressure and shear strain responses in the soil deposit is facilitated using appropriate and calibrated instruments. The instrumented array at UT-2 consisted of eight, custom triaxial geophone packages (designated 1G through 8G; Figures 1 and 2) to measure the particle velocity and three pore pressure transducers (1PPT through 3PPT) were installed using direct-push methods to their selected depths and positions. The orientation of each geophone was aligned with one another and included one component parallel and perpendicular to the direction of uniaxial shaking. Four crosshole source rods (1R through 4R; Figures 1 and 2) were advanced to the depth corresponding to a given geophone pair, the latter of which provided a crosshole distance of 0.9 m between the rod and geophone. The source rods and geophones facilitated observation of V_p and V_s prior to and following a given shaking event.

After installation of the instruments, the vibroseis was positioned over the center of array and the 2.3 m square base plate lowered to engage and couple with the ground surface under its dead weight (approximately 29,000 kg). The *in-situ* testing program consists of seven stages of sinusoidal horizontal shear loading applied at a frequency of 10 Hz and for N = 40, except for Stage 7 which included N = 100. The variation of excess pore pressure was continuously monitored using PPTs during the initial consolidation period and after each loading stage to ensure that full dissipation occurred prior to applying a given loading stage. In each loading stage the magnitude of dynamic loading was sequentially increased to evaluate the pore pressure response and nonlinear behavior over a wide range of strain magnitudes.

The triaxial displacement time histories for each geophone package were calculated by performing numerical integration of the particle velocity time history. Then, the shear strain time-history within the sensor array was calculated using two-dimensional isoparametric finite elements with appropriate shape functions following the procedure proposed by Rathje et al. (2004), Cox et al. (2009), and others. The average shear strain thus calculated corresponded to the location of the PPTs and may be compared to the excess pore pressure observed during each loading stage.

4.2 *Results from In-situ Mobile Shaking*

The calculated Cauchy shear strain in the xz plane, γ_{xz}, where z = depth and x = the horizontal direction parallel to the direction of loading, ranged from 0.001% to 0.261%, increasing with the increased cyclic loading amplitude and decreasing with depth. Excess pore pressures were initiated during Stage 3, with γ_{xz} = 0.009% for 2PPT (z = 2 m), whereas 1PPT and 3PPT registered excess pore pressures during Stages 5 and 6 with γ_{xz} = 0.055 and 0.061%, respectively. The strong variation in the depth-dependent excess pore pressure response is indicative of the variability in consistency, stiffness, and cyclic strength with depth at UT-2 (Figure 1). Figure 4 illustrates the variation of γ_{xz} and excess pore pressure ratio, r_u, versus the number of loading cycles, N, for the 6th and 7th Stages of loading and for 2PPT. The average T-Rex-induced γ_{xz} over 40 loading cycles is about 0.082% corresponding to $r_{u,max}$ and $r_{u,r}$ of 0.261 and 0.162% for Stage 6 (Figure 4a). Upon termination of the cyclic loading and attenuation of the seismic signal, r_u continued to increase due to migration of larger excess pore pressures from the adjacent soil volume, indicating that a 3D hydraulic gradient had been established as a result of the loading sequence. A similar response can be observed for the 7th and last stage of loading, which was conducted with N = 100. Loading Stage 7 (Figure 4b) produced an average γ_{xz} = 0.175%, with $r_{u,max}$ and $r_{u,r}$ of 0.61 and 0.18%, and 1.46 and 1.16% at N = 40 and 100, respectively.

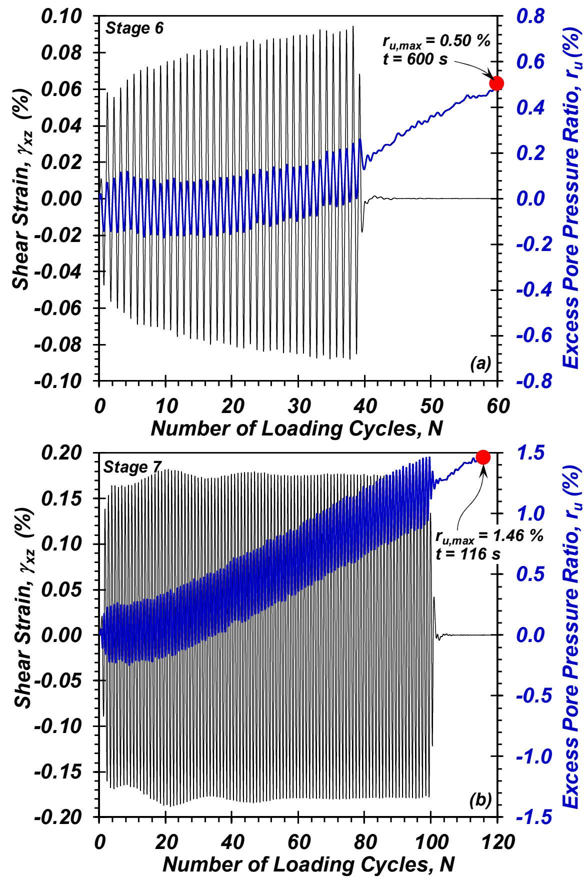

Figure 4. Shear strain and excess pore pressure ratio time histories for T-Rex loading and the 2PPT position at 2 m depth: (a) Stage 6, N = 40, and (b) Stage 7, N = 100.

4.3 *Comparison to Laboratory Test Results and Discussion*

Figure 5a presents the variation of $r_{u,r}$ versus shear strain deduced from the *in-situ* T-Rex loading and strain-controlled DSS tests on intact specimens from comparable depths. For the purposes of comparison, *in-situ* Cauchy shear strains were converted to DSS-equivalent shear strains using the procedure described by Jana and Stuedlein (2021b, 2021c). Generally, the increasing trend of $r_{u,r}$ with shear strain for the laboratory and *in-situ* loading are in agreement with one another, although differences are noted. The *in-situ* test results indicate that $\gamma_{tp} \approx$ 0.03% and 0.01% for depths of 1.5 and 2.0 m, respectively, compared to $\gamma_{tp} \approx$ 0.01 to 0.02% from the DSS tests at ~1.45 m, indicating good agreement. However, the variation of $r_{u,r}$ with γ was smaller *in-situ* than in the DSS tests. The *in-situ* and DSS test-derived γ_{tp} is consistent with previous laboratory tests on intact natural plastic soils

(Tabata and Vucetic 2010). The observed differences in the excess pore pressure response may stem from the differing boundary conditions in the laboratory and *in-situ* conditions; for example, the constant-volume boundary in the DSS tests approximate undrained conditions, whereas volumetric strains are not restrained *in-situ,* similar to the condition during earthquake loading. However, there are also notable differences in the saturation conditions between 1.5 and 2.0 m. The *in-situ* V_p at 1.5 m depth was 277 m/s, whereas at 2.0 m depth V_p = 838 m/s. Generally, V_p > 700 m/s indicates nearly fully-saturated conditions, as observed by Stokoe et al. (2016) and Jana and Stuedlein (2021a). Note that the natural, intact DSS test specimens exhibited, V_p = 1,162 and 1,213 m/s with S_r = ~100% (Table 1), and the cyclic resistance of partially-saturated silty soils can be significantly larger than that at the fully-saturated state (Okamura and Noguchi 2009; Stokoe et al. 2014), all other variables held constant. Finally, the role of inherent variability of the soils and differences in response between the small DSS test specimens and the large soil volume loaded *in-situ* cannot be ignored in the subtle differences in the observed responses.

Figure 5b compares the G/G_{max} curves derived from laboratory test specimens to that from the *in-situ* tests. Two sets of G/G_{max} curves are presented: those conducted at the previously-mentioned loading frequencies, and the same data corrected to 1 Hz loading frequency as suggested by Vardanega and Bolton (2013) to provide a common basis for comparison. The RCTS and *in-situ* test results agree fairly well up to $\gamma \approx$ 0.05%, upon which stronger nonlinearity in the *in-situ* response is observed, due in part to the greater number of cycles associated with the T-rex loading protocol as well as differences in S_r for the two depths compared Generally, these two experimentally-derived sets of G/G_{max} curves compare favorably against those proposed by Vucetic and Dobry (1991) for plastic soils within the range of PI in proximity to that at UT-2. On the contrary, the DSS test results exhibited higher reduction in G than the RCTS and *in-situ* test data within the medium strain range (0.01% < γ < 0.3%), which is likely due to both compliance and differences in S_r. Improved agreement appears possible at larger strains.

5 CONCLUSIONS

Advances in *in-situ* testing have served to further bridge the gap between the dynamic performance of large volumes of soil and laboratory test results derived from small specimens subjected to idealized boundary conditions. This paper presents the comparison of cyclic soil responses derived for an instrumented array within a deposit of alluvial silt and two available laboratory tests. The alluvial silt deposit exhibited spatially-variable soil properties (e.g., S_r) that served to explain several differences observed in the generation of excess pore pressure and nonlinearity in shear modulus. The *in-situ* shear strain-excess pore pressure response for the instrumented depth corresponding to nearly-saturated conditions and the saturated direct simple shear test specimens exhibited similar threshold shear strains to trigger excess pore pressures when compared on a common shear strain basis, the DSS-equivalent shear strain. On the other hand, the strain rate-corrected *in-situ* shear modulus reduction behavior was most comparable to the resonant column-torsional shear test specimen up to $\gamma \approx$ 0.05%. Additional comparisons of other test panels at the Port of Longview property are underway and will serve to further advance our understanding of the similarities and differences of laboratory and *in-situ* cyclic behavior of silty soils.

6 ACKNOWLEDGEMENTS

The work described in this paper was funded by the National Science Foundation (NSF) Grants CMMI 1663654, CMMI 1663531, and CMMI 1520808. The findings presented herein represent that of the authors and do not necessarily represent views of NSF. The authors would also like to express their gratitude to the Port of Longview, Longview, WA and their employees for providing and coordinating access to the test site.

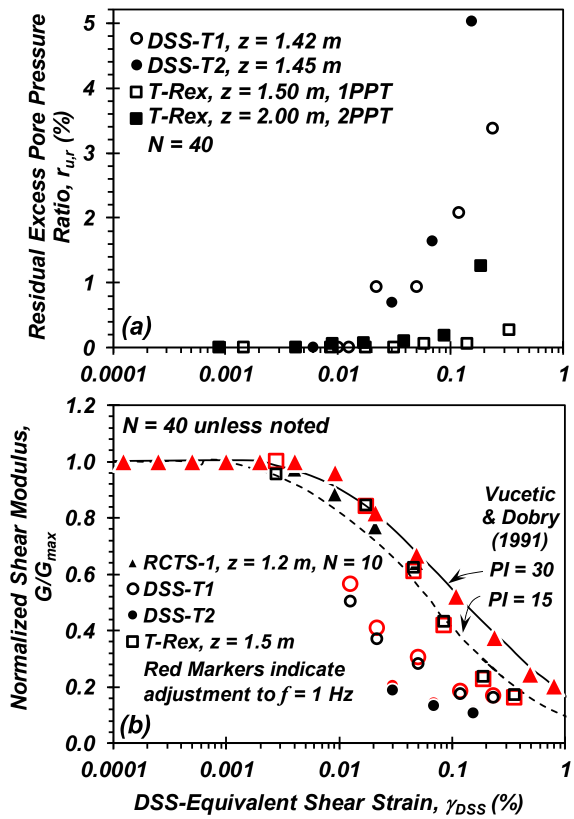

Figure 5. Comparison of *in-situ* and laboratory-derived variation of (a) residual excess pore pressure ratio, $r_{u,r}$ and (b) shear modulus reduction, G/G_{max}, with shear strain.

7 REFERENCES

Adamidis, O., and S. P. G. Madabhushi. 2018. “Experimental investigation of drainage during earthquake-induced liquefaction.” Géotechnique 68 (8): 655–665. https://doi.org/10.1680/jgeot.16.P.090.

Cox, B. R. 2006. Development of a direct test method for dynamically assessing the liquefaction resistance of soils in situ. *PhD Thesis*, University of Texas, Austin, TX.

Cox, B. R., Stokoe, K. H., and Rathje, E. M. 2009. An in situ test method for evaluating the coupled pore pressure generation and nonlinear shear modulus behavior of liquefiable soils. *Geotech. Test. J.*, 32(1), 11-21.

Cox, B. R., Stolte, A. C., Stokoe, K. H., & Wotherspoon, L. M. (2018). A Direct-Push Crosshole (DPCH) Test Method for the In Situ Evaluation of High-Resolution P-and S-Wave Velocities. *Geotech. Test. J.*, 42(5), 1101-1132.

Cubrinovski, M., Rhodes, A., Ntritsos, N., and Van Ballegooy, S. 2019. System response of liquefiable deposits. *Soil Dyn. Earthq. Eng.*, 124, 212-229.

Hsu, C.C. and Vucetic, M. 2006. Threshold shear strain for cyclic pore-water pressure in cohesive soils. *J. Geotech. Geoenv. Eng.*, 132(10):1325-1335.

Ichii, K., & Mikami, T. 2018. Cyclic threshold shear strain in pore water pressure generation in clay in situ samples. *Soils Found.*, 58(3): 756-765.

Jana, A. and Stuedlein, A.W. (2021a). Monotonic, Cyclic and Post-Cyclic Response of an Alluvial Plastic Silt Deposit. *J. Geotech. Geoenviron. Eng*, 147(3), 04020174.

Jana, A. and Stuedlein, A.W. (2021b). Dynamic, In-situ, Nonlinear-Inelastic Response and Post-Cyclic Strength of a Plastic Silt Deposit. *Can. Geotech. J.*, http://dx.doi.org/10.1139/cgj-2020-0652

Jana, A. and Stuedlein, A.W. (2021c). Dynamic, In-situ, Nonlinear-Inelastic Response of a Deep, Medium Dense Sand Deposit. *J. Geotech. Geoenv. Eng.*, Vol. 147, No. 6, pp. 04021039.

Kurtulus, A., and Stokoe, K. H. (2008). In situ measurement of nonlinear shear modulus of silty soil. *J. Geotech. Geoenv. Eng*, 134(10): 1531-1540.

Mortezaie, A. and Vucetic, M., 2016. Threshold shear strains for cyclic degradation and cyclic pore water pressure generation in two clays. *J. Geotech. Geoenviron. Eng.*, 142(5): 04016007.

Okamura, M., and Noguchi, K. (2009). Liquefaction resistances of unsaturated non-plastic silt. *Soils and Foundations*, 49(2), 221-229.

Rathje, E. M., Chang, W.-J., Stokoe, K. H., and Cox, B. 2004. Evaluation of ground strain from in situ dynamic response. *Proc., 13th World Conf. Earthq. Eng.*, Vancouver, BC.

Roberts, J.N., Stokoe, K.H., II, Hwang, S., Cox, B.R., Wang, Y., Menq, F.M., and van Ballegooy, S. 2016, Field measurements of the variability in shear strain and pore pressure generation in Christchurch soils, *In Proc., 5th Int. Conf. on Geotech. Geophys. Site Char.*, ICS5, Sydney, Australia.

Robertson, P. K. (1990). Soil classification using the cone penetration test. Canadian geotechnical journal, 27(1), 151-158.

Robertson, P. 2009. Interpretation of cone penetration tests – a unified approach. *Can. Geotech. J.*, 46(11): 1337–1355.

Stokoe, II, K.H., Roberts, J.N., Hwang, S., Cox, B.R., Menq, F.Y., Van Ballegooy, S. 2014. Effectiveness of inhibiting liquefaction triggering by shallow ground improvement methods: initial field shaking trials with T-Rex at one site in Christchurch. Soil Liquefaction During Recent Large-Scale Earthquakes, Orense, Towhata & Chouw (Eds.), Taylor & Francis Group, London.

Stokoe K.H., Roberts J.N., Hwang S., Cox B.R., and Menq F. (2016), Effectiveness of inhibiting liquefaction triggering by shallow ground improvement methods: field shaking trials with T-Rex at one area in Christchurch, New Zealand. *24th Geot. Conf. of Torino, Turin, Italy*.

Tabata, K., and Vucetic, M. 2010. Threshold shear strain for cyclic degradation of three clays. *Proc., 5th Int. Conf. Recent Advanecs in Geotech. Earthq. Eng. Soil Dyn.*, San Diego, CA.

Van Ballegooy, S., Roberts, J. N., Stokoe, K. H., Cox, B. R., Wentz, F. J., and Hwang, S. 2015. Large-scale testing of shallow ground improvements using controlled staged-loading with T-Rex. *Proc., 6th Int. Conf. Earthq. Geotech. Eng.*, Christchurch, NZ.

Vardanega, P. J., and Bolton, M. D. 2013. Stiffness of clays and silts: Normalizing shear modulus and shear strain. *J. Geotech. Geoenviron. Eng*, 139(9), 1575-1589.

Vucetic, M., and Dobry, R. (1991). Effect of soil plasticity on cyclic response. *J. of Geotech. Eng.*, 117(1), 89-107.

Wijewickreme, D., A. Soysa, and P. Verma. 2019. Response of Natural Fine-Grained Soils for Seismic Design Practice. *Soil Dyn. Earthq. Eng.*, 124: 280-296.